Dynamic Response of a Cylinder to a Side Pressure Pulse

JOHN S. HUMPHREYS* AND ROBERT WINTER†
Avco Corporation, Wilmington, Mass.

An analysis of the elastic vibration of an isotropic, infinitely long cylindrical shell under a transverse pressure pulse using a linearized, small deformation theory is presented. Two cases of a pressure pulse decreasing linearly with time, distributed as a cosine over half the circumference and constant along the length of the cylinder, are considered, one with a positive phase only and one with an equal negative phase (zero total impulse). The analysis neglects transverse stresses and makes use of the thin-shell assumption of a linear stress distribution across the thickness to determine the maximum in-plane stresses. The solutions for displacements are in the form of infinite series, and computer calculations of the associated maximum stress levels have been performed for some representative cases of interest, truncating the series at 200 terms. Among the general conclusions that can be drawn from the results is that, for pressure pulses of relatively short duration times (less than 0.1 radius/sound speed), the response essentially depends only on the total impulse and is independent of the pulse shape. It is also seen that bending effects play a rather small role in terms of affecting the maximum stresses reached, particularly for early times, where a pure membrane solution gives a very close approximation (even for a thickness-to-radius ratio as high as 0.05).

Nomenclature

a = radius to midsurface of undeformed cylinder
a_n = coefficient of Fourier series
c = $[E/(1-\nu^2)\rho]^{1/2}$ speed of sound in material
E = elastic modulus of material
h = thickness of cylinder wall
I = peak impulse per unit area
$\bar{I}$ = $[c(1-\nu^2)I]/Eh$, dimensionless impulse per unit area
M = circumferential bending moment resultant
N = circumferential force resultant
p = applied pressure
$\bar{P}$ = $[a(1-\nu^2)p]/Eh$, dimensionless pressure
t = time
t_1 = time duration of pulse
v = circumferential deformation of midsurface
w = inward radial deformation of midsurface
z = radial distance from midsurface
α^2 = $h^2/12a^2$, geometric parameter
β_n, γ_n = dimensionless frequencies
ζ = w/a, dimensionless inward radial deformation of middle surface
θ = angular coordinate of undeformed cylinder
ν = Poisson's ratio of material
ρ = mass density of material
σ = circumferential stress
$\bar{\sigma}$ = $\sigma h/Ic$, dimensionless circumferential stress
τ = ct/a, dimensionless time
τ_1 = dimensionless time duration of pulse
ψ = angular displacement of middle surface

I. Introduction and Problem Formulation

An analysis is presented of the elastic vibration of an isotropic, infinitely long cylindrical shell under a transverse pressure pulse using a linearized, small deformation theory. This pressure pulse is assumed to be distributed as a cosine over half the circumference and to be constant along the length of the cylinder, independent of its distribution in time. The analysis neglects transverse stresses and makes use of the thin-shell assumption of a linear stress distribution across the thickness to determine the maximum in-plane stresses.

Using plane-strain Hookes law relations and neglecting the radial stress, there remains only one independent normal stress component in the circumferential direction (the axial normal stress can be obtained by multiplying this stress by Poisson's ratio). The circumferential force and moment resultants N and M are defined in terms of the circumferential normal stress σ by

$$N = -\int_{-h/2}^{h/2} \sigma dz \tag{1a}$$

$$M = \int_{-h/2}^{h/2} z\sigma dz \tag{1b}$$

If all displacements, derivatives and motion in the axial direction are neglected, and terms in h^2/a^2 are dropped compared to 1, the complete linear shell theory equations of motion in terms of displacements u, v, w are (from Flugge,[1] adding inertia terms and changing to present notation)

$$\left.\begin{aligned} &\frac{\partial v}{\partial \theta} - w + \frac{h^2}{12a^2}\left[-\frac{\partial^4 w}{\partial\theta^4} - 2\frac{\partial^2 w}{\partial\theta^2}\right] = -\frac{\rho h a^2}{D}\frac{\partial^2 w}{\partial t^2} + \frac{pa^2}{D} \\ &\frac{\partial^2 v}{\partial\theta^2} - \frac{\partial w}{\partial\theta} = \frac{\rho h a^2}{D}\frac{\partial^2 v}{\partial t^2} \end{aligned}\right\} \tag{2}$$

where

$$D = \frac{Eh}{1-\nu^2}$$

with associated force-displacement relations

$$\begin{aligned} M &= \frac{Eh^3}{12(1-\nu^2)a}\left(\frac{\partial^2 w}{\partial\theta^2} + w\right) \\ N &= \frac{Eh}{a(1-\nu^2)}\left(\frac{h^2}{12a^2}\frac{\partial^2 w}{\partial\theta^2} + w - \frac{\partial v}{\partial\theta}\right) \end{aligned} \tag{3}$$

Over-all geometry and definitions of positive v, w, M, and N

Presented at the AIAA Fifth Annual Structures and Materials Conference, Palm Springs, Calif., April 1–3, 1964 (no preprint number; published in bound volume of preprints of the meeting); revision received September 15, 1964. The helpful suggestions of R. G. Payton during this work and the assistance of C. Berndtson with the numerical computations are greatly appreciated.

* Senior Staff Scientist, Research and Advanced Development Division. Member AIAA.
† Associate Scientist, Research and Advanced Development Division. Member AIAA.

are given in Fig. 1. Nondimensional variables are now introduced as follows;

$$\zeta = w/a \tag{4}$$

$$\psi = v/a \tag{5}$$

$$\tau = \frac{ct}{a} = \left[\frac{E}{(1-\nu)^2\rho}\right]^{1/2}\frac{t}{a} \tag{6}$$

$$\alpha^2 = h^2/12a^2 \tag{7}$$

If these are used in (2), the basic differential equations become

$$\alpha^2\frac{\partial^2}{\partial\theta^2}\left(\frac{\partial^2\zeta}{\partial\theta^2} + 2\zeta\right) + \zeta - \frac{d\psi}{\partial\theta} + \frac{\partial^2\zeta}{\partial\tau^2} = \bar{P}(\theta,\tau) \tag{8a}$$

$$\frac{\partial}{\partial\theta}\left(\zeta - \frac{\partial\psi}{\partial\theta}\right) + \frac{\partial^2\psi}{\partial\tau^2} = 0 \tag{8b}$$

where $\bar{P}$ is a nondimensional pressure, defined as

$$\bar{P}(\theta,\tau) = \frac{a(1-\nu^2)}{Eh}p(\theta,\tau) \tag{9}$$

The initial (rest) conditions are

$$\zeta(\theta,0) = \psi(\theta,0) = \frac{\partial\zeta}{\partial\tau}(\theta,0) = \frac{\partial\psi}{\partial\tau}(\theta,0) = 0 \tag{10}$$

and the elastic law relations (3) become

$$\frac{(1-\nu^2)}{Eha}M(\theta,\tau) = \alpha^2\left(\frac{\partial^2\zeta}{\partial\theta^2} + \zeta\right) \tag{11a}$$

$$\frac{(1-\nu^2)}{Eh}N(\theta,\tau) = \alpha^2\frac{\partial^2\zeta}{\partial\theta^2} + \zeta - \frac{\partial\psi}{\partial\theta} \tag{11b}$$

These basic linear equations, (8) and (11), are also derived in the course of a more extensive nonlinear analysis by Goodier and McIvor.[2]

II. General Problem Solution

If only those loadings that are symmetric about $\theta = 0$ and that can be represented in a separated variable form (with a Fourier cosine series in space) are considered, then

$$\bar{P}(\theta,\tau) = P(\tau)\left(a_0 + \sum_{n=1}^{\infty} a_n \cos n\theta\right) \tag{12}$$

where $P(\tau)$ is an arbitrary time function.

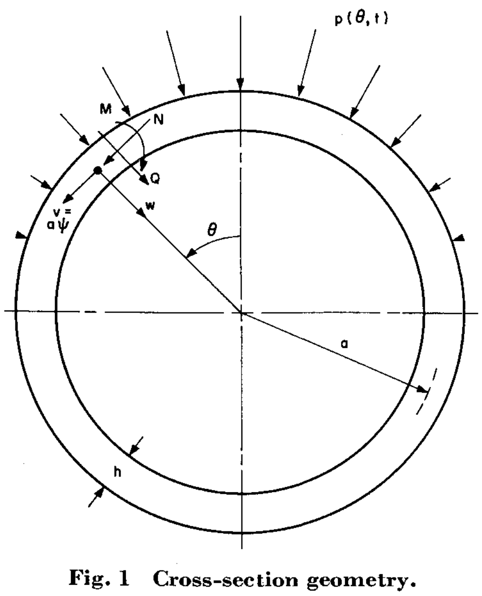

Fig. 1 Cross-section geometry.

The general Fourier series expansions for ζ and ψ reduce, in this symmetric case, to

$$\zeta = \zeta_0(\tau) + \sum_{n=1}^{\infty}\zeta_n(\tau)\cos n\theta \tag{13a}$$

$$\psi = \sum_{n=1}^{\infty}\psi_n(\tau)\sin n\theta \tag{13b}$$

so that Eqs. (8) become

$$\zeta_0 + \ddot{\zeta}_0 + \sum_{n=1}^{\infty}\{[\alpha^2(n^2-1)^2+1]\zeta_n - n\psi_n + \ddot{\zeta}_0\}\cos n\theta = P(\tau)\left(a_0 + \sum_{n=1}^{\infty} a_n\cos n\theta\right) \tag{14a}$$

$$\sum_{n=1}^{\infty}(n^2\psi_n - n\zeta_n + \ddot{\psi}_n)\sin n\theta = 0 \tag{14b}$$

using the dot notation for $\partial/\partial\tau$.

The coefficients of $\cos n\theta$ and $\sin n\theta$ must vanish independently for every n. Thus, when $n = 0$

$$\zeta_0 + \ddot{\zeta}_0 = a_0P(\tau) \tag{15}$$

When $n \geq 1$

$$[\alpha^2(n^2-1)^2+1]\zeta_n - n\psi_n + \ddot{\zeta}_n = a_nP(\tau) \tag{16a}$$

$$n\psi_n - n\zeta_n + \ddot{\psi}_n = 0 \tag{16b}$$

Eliminating ζ_n in Eqs. (16), and rearranging terms,

$$\ddot{\ddot{\psi}}_n + [\alpha^2(n^2-1)^2 + n^2 + 1]\ddot{\psi}_n + \alpha^2n^2(n^2-1)^2\psi_n = na_nP(\tau) \tag{17}$$

Using a standard single-sided Laplace transform approach, the transforms of the ψ_n and ζ_n can be written as products of known functions and the arbitrary $P(\tau)$. Inverse transforms of these known functions are then found from Erdelyi,[3] and use of the convolution theorem gives

$$\psi_n(\tau) = na_n\int_0^{\tau}\left[\frac{\sin\gamma_n(\tau-x)}{Q_n\gamma_n} - \frac{\sin\beta_n(\tau-x)}{Q_n\beta_n}\right]P(x)dx \tag{18a}$$

$$\zeta_n(\tau) = \frac{a_n}{Q_n}\int_0^{\tau}\left[\left(\frac{n^2}{\gamma_n} - \gamma_n\right)\sin\gamma_n(\tau-x) - \left(\frac{n^2}{\beta_n} - \beta_n\right)\sin\beta_n(\tau-x)\right]P(x)dx \tag{18b}$$

where

$$\gamma_n^2 = \tfrac{1}{2}(\alpha^2n^4 + n^2 + 1) + \tfrac{1}{2}[\alpha^4n^8 - 2\alpha^2n^6 + (n^2+1)^2]^{1/2} \tag{19a}$$

$$\beta_n^2 = \tfrac{1}{2}(\alpha^2n^4 + n^2 + 1) - \tfrac{1}{2}[\alpha^4n^8 - 2\alpha^2n^6 + (n^2+1)^2]^{1/2} \tag{19b}$$

$$Q_n = \beta_n^2 - \gamma_n^2 = -[\alpha^4n^8 - 2\alpha^2n^6 + (n^2+1)^2]^{1/2} \tag{19c}$$

and α^2 has been neglected compared with unity.

From Eq. (15), using the same transform approach, the initial term is directly

$$\zeta_0(\tau) = a_0\int_0^{\tau}\sin(\tau-x)P(x)dx \tag{20}$$

If a linear stress distribution is assumed, then the extreme values at $z = \pm h/2$ are

$$\sigma_{\pm h/2} = -(N/h) \pm (6M/h^2) \tag{21}$$

Solutions for M and N are given by substituting Eqs. (13) into (11):

$$M = \frac{Eha\alpha^2}{1-\nu^2}\sum_{n=0}^{\infty}\zeta_n(1-n^2)\cos n\theta \tag{22a}$$

$$N = \frac{Eh}{1-\nu^2}\sum_{n=0}^{\infty}[\zeta_n(1-\alpha^2n^2) - n\psi_n]\cos n\theta \quad (22b)$$

Thus (21) becomes

$$\frac{(1-\nu^2)}{E}\sigma_{\pm h/2} = \sum_{n=0}^{\infty}\left\{n\psi_n + \left[\alpha^2n^2 - 1 \pm \frac{h}{2a}(1-n^2)\right]\zeta_n\right\}\cos n\theta \quad (23)$$

All that remains is to choose a pressure function $\bar{P}(\theta, \tau)$ and, using it in Eq. (18), find ψ_n and ζ_n and solve for $\sigma_{\pm h/2}$ from (23).

III. Results for Specific Loading Pulses

A. Positive Impulse Loading

Any arbitrary pressure time function can be chosen. The first specific pressure pulse being considered is assumed to decrease linearly with time from a peak value p_0 to zero with a time duration t_1 (see Fig. 2):

$$p(t) = p_0[1 - (t/t_1)] \qquad 0 < t < t_1$$
$$= 0 \qquad t > t_1$$

Defining a nondimensional impulse per unit area

$$\bar{I} = \frac{Ic(1-\nu^2)}{Eh} = \frac{1}{2}p_0\tau_1 \quad (24)$$

where

$$I = \int_0^{t_1} p(t)dt = \tfrac{1}{2}p_0t_1$$

then

$$P(\tau) = \frac{2\bar{I}}{\tau_1}\left(1 - \frac{\tau}{\tau_1}\right) \qquad 0 \le \tau \le \tau_1$$
$$= 0 \qquad \tau > \tau_1 \quad (25)$$

The pulse is assumed to be distributed, in space, over half the circumference in a cosine form (see Fig. 2):

$$\bar{P}(\theta,\tau) = P(\tau)\cos\theta \qquad -(\pi/2) \le \theta \le (\pi/2)$$
$$= 0 \qquad |\theta| > (\pi/2) \quad (26)$$

Coefficients for the Fourier series expansion for $\bar{P}(\theta, \tau)$ [see (12)] are given by

$$\left.\begin{aligned} a_0 &= 1/\pi \\ a_1 &= \tfrac{1}{2} \\ a_n &= -\frac{2(-1)^{n/2}}{\pi(n^2-1)} \qquad n = 2, 4, 6, \ldots \\ &= 0 \qquad n = 3, 5, 7, \ldots \end{aligned}\right\} \quad (27)$$

Expressions for $\psi_n(\tau)$, $\zeta_n(\tau)$, and $\zeta_0(\tau)$ are found using (25) and (27) in (18) and (20), separate solutions for $\tau < \tau_1$ and $\tau > \tau_1$ being necessary due to the convolution integrals involved.

For $\tau \le \tau_1$

$$\psi_n(\tau) = \frac{2\bar{I}na_n}{\tau_1Q_n}\left[\frac{1}{\gamma_n^2}\left(1 - \frac{\tau}{\tau_1} - \cos\gamma_n\tau + \frac{\sin\gamma_n\tau}{\tau_1\gamma_n}\right) - \frac{1}{\beta_n^2}\left(1 - \frac{\tau}{\tau_1} - \cos\beta_n\tau + \frac{\sin\beta_n\tau}{\tau_1\beta_n}\right)\right] \quad (28a)$$

$$\zeta_0(\tau) = \frac{2\bar{I}a_0}{\tau_1}\left(1 - \cos\tau - \frac{\tau}{\tau_1} + \frac{\sin\tau}{\tau_1}\right) \quad (28b)$$

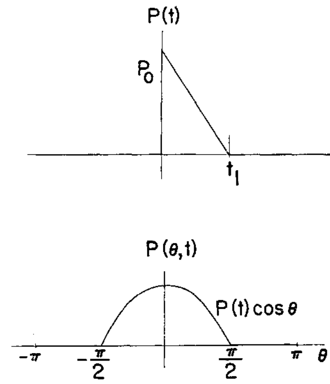

Fig. 2 Pressure loading as a function of time and space.

$$\zeta_n(\tau) = \frac{2\bar{I}a_n}{\tau_1Q_n}\left[\left(\frac{n^2}{\gamma_n^2} - 1\right)\left(1 - \frac{\tau}{\tau_1} - \cos\gamma_n\tau + \frac{\sin\gamma_n\tau}{\tau_1\gamma_n}\right) - \left(\frac{n^2}{\beta_n^2} - 1\right)\left(1 - \frac{\tau}{\tau_1} - \cos\beta_n\tau + \frac{\sin\beta_n\tau}{\tau_1\beta_n}\right)\right] \quad (28c)$$

For $\tau > \tau_1$

$$\psi_n(\tau) = \frac{2\bar{I}na_n}{\tau_1Q_n}\left[\left(\frac{1-\cos\gamma_n\tau_1}{\gamma_n\tau_n}\right)\frac{\sin\gamma_n\tau}{\gamma_n^2} - \left(1 - \frac{\sin\gamma_n\tau_1}{\gamma_n\tau_1}\right)\frac{\cos\gamma_n\tau}{\gamma_n^2} - \left(\frac{1-\cos\beta_n\tau_1}{\beta_n\tau_1}\right)\frac{\sin\beta_n\tau}{\beta_n^2} + \left(1 - \frac{\sin\beta_n\tau_1}{\beta_n\tau_1}\right)\frac{\cos\beta_n\tau}{\beta_n^2}\right] \quad (29a)$$

$$\zeta_0(\tau) = \frac{2\bar{I}a_0}{\tau_1}\left[\left(\frac{1-\cos\tau_1}{\tau_1}\right)\sin\tau - \left(1 - \frac{\sin\tau_1}{\tau_1}\right)\cos\tau\right] \quad (29b)$$

$$\zeta_n(\tau) = \frac{2\bar{I}a_n}{\tau_1Q_n}\left[\left(\frac{1-\cos\gamma_n\tau_1}{\gamma_n\tau_1}\right)\left(\frac{n^2}{\gamma_n^2} - 1\right)\sin\gamma_n\tau - \left(1 - \frac{\sin\gamma_n\tau_1}{\gamma_n\tau_1}\right)\left(\frac{n^2}{\gamma_n^2} - 1\right)\cos\gamma_n\tau - \left(\frac{1-\cos\beta_n\tau_1}{\beta_n\tau_1}\right)\left(\frac{n^2}{\beta_n^2} - 1\right)\sin\beta_n\tau + \left(1 - \frac{\sin\beta_n\tau_1}{\beta_n\tau_1}\right)\left(\frac{n^2}{\beta_n^2} - 1\right)\cos\beta_n\tau\right] \quad (29c)$$

When these quantities are substituted into (23) using (27), the impulse I is transferred to the left-hand side, and terms are rearranged; the final expression for the maximum dimensionless stress is obtained. For $\tau > \tau_1$, after the pulse has vanished (which is the region of interest for short pulses),

$$\bar{\sigma}_{\pm} \equiv \frac{h}{Ic}\sigma_{\pm h/2} = \frac{2}{\pi}\left\{\left(\pm\frac{h}{2a} - 1\right) \times \left[\left(\frac{1-\cos\tau_1}{\tau_1^2}\right)\sin\tau - \frac{1}{\tau_1}\left(1 - \frac{\sin\tau_1}{\tau_1}\right)\cos\tau\right] - \frac{\pi}{4}\left[\left(\frac{1-\cos 2^{1/2}\tau_1}{2^{1/2}\tau_1^2}\right)\sin 2^{1/2}\tau - \frac{1}{\tau_1}\left(1 - \frac{\sin 2^{1/2}\tau_1}{2^{1/2}\tau_1}\right)\times \cos 2^{1/2}\tau\right]\cos\theta - 2\sum_{n=2,4,6\ldots}^{\infty}\frac{(-1)^{n/2}}{(n^2-1)Q_n}[q_{n\pm}(A_{2n}\sin\gamma_n\tau - A_{1n}\cos\gamma_n\tau) - r_{n\pm}(B_{2n}\sin\beta_n\tau - B_{1n}\cos\beta_n\tau)]\right\} \quad (30)$$

where

$$A_{1n} = \frac{\gamma_n\tau_1 - \sin\gamma_n\tau_1}{\gamma_n\tau_1^2} \qquad A_{2n} = \frac{1-\cos\gamma_n\tau_1}{\gamma_n\tau_1^2}$$

$$B_{1n} = \frac{\beta_n\tau_1 - \sin\beta_n\tau_1}{\beta_n\tau_1^2} \qquad B_{2n} = \frac{1-\cos\beta_n\tau_1}{\beta_n\tau_1^2}$$

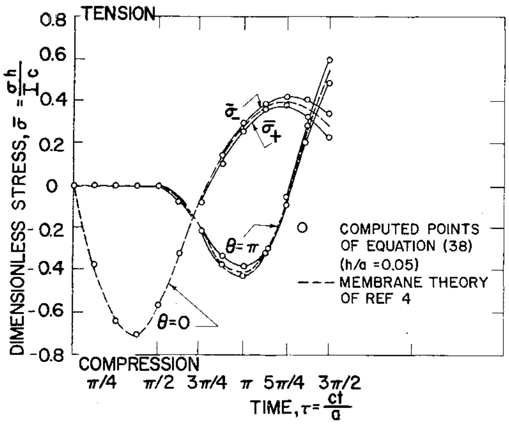

Fig. 3 Results compared to membrane theory of Payton[4] for pure impulse ($\tau_1 = 0$).

$$q_{n\pm} = 1 + \left(\frac{n^2}{\gamma_n{}^2} - 1\right)\left[\frac{h^2n^2}{12a^2} \pm \frac{h}{2a}(1 - n^2)\right]$$

$$r_{n\pm} = 1 + \left(\frac{n^2}{\beta_n{}^2} - 1\right)\left[\frac{h^2n^2}{12a^2} \pm \frac{h}{2a}(1 - n^2)\right]$$

γ_n, β_n, and Q_n are defined in Eqs. (19) and $(1 - \nu^2)/(\bar{I}E) = h/Ic$.

Considering the limiting condition in which the impulse remains constant while its time of action approaches zero, Eq. (30) becomes

$$\bar{\sigma}_{\pm} = \frac{1}{\pi}\left(\pm\frac{h}{2a} - 1\right)\sin\tau - \frac{2^{1/2}}{4}\sin 2^{1/2}\tau\cos\theta - \frac{2}{\pi}\sum_{n=2,4\ldots}^{\infty}\frac{(-1)^{n/2}}{(n^2-1)Q_n}(q_{n\pm}\gamma_n\sin\gamma_n\tau - r_{n\pm}\beta_n\sin\beta_n\tau)\cos n\theta \quad (31)$$

This "impulsive loading" case has been calculated for comparison to a paper by Payton,[4] as shown in Fig. 3. It is of interest that Payton's membrane solution agrees almost exactly at very early times with the present solution including bending terms. Bending effects become noticeable only after the first cycle of stress.

The terms of the full equation (30) have been calculated and summed to $n = 400$ (200 terms in the series) on a digital computer for time $\tau \leq 4\pi$, position $\theta = 0$, $\pi/2$, and π, and for the parameter values $h/a = 0.01$, 0.02, 0.05, 0.10, and $\tau_1 = 0, 0.0001, 0.001, 0.01, 1.0, 2, 4$, and 10 (not in all possible combinations). For metal cylinders with a radius of about

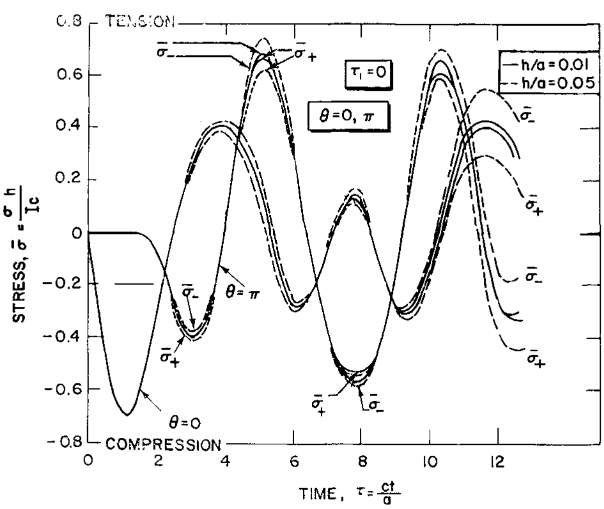

Fig. 4 Computed cylinder response, impulsive loading, ($\theta = 0, \pi$).

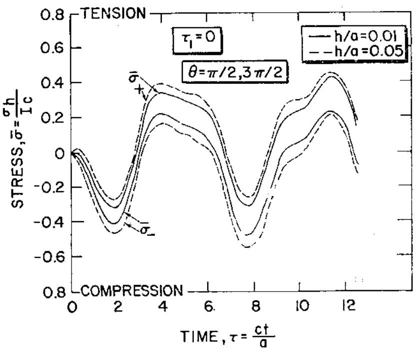

Fig. 5 Computed cylinder response, impulsive loading, ($\theta = \pi/2, 3\pi/2$).

1 ft, a τ_1 of 0.01 corresponds very roughly to 1 μsec. It was found that numerical difficulties were encountered with terms such as $\sin\gamma_n\tau_1/\gamma_n\tau_1$ because of the small argument values being considered, and so it was necessary to expand such terms in a Taylor's series approximation for these small values of the argument. In this way, it was also possible to compute a value for the limiting case of $\tau_1 = 0$, corresponding to Eq. (31), from the same program. With this modification in the calculation, it was found by looking closely at a few specific cases that convergence to three-figure accuracy is generally obtained by taking between 10 and 30 terms in the series; the higher the value of τ_1, the more terms are required. The inner and outer fiber stresses, ($\bar{\sigma}_-$ and $\bar{\sigma}_+$) of Eq. (30), are shown plotted in Figs. 4–7 as a function of time and position for τ_1 and 1.0 and $h/a = 0.01$ and 0.05.

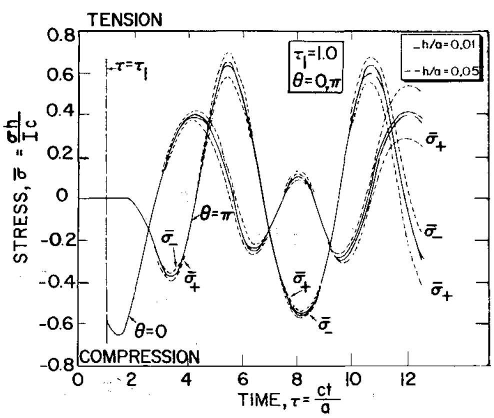

Fig. 6 Computed cylinder response, finite pulse time, ($\theta = 0, \pi$).

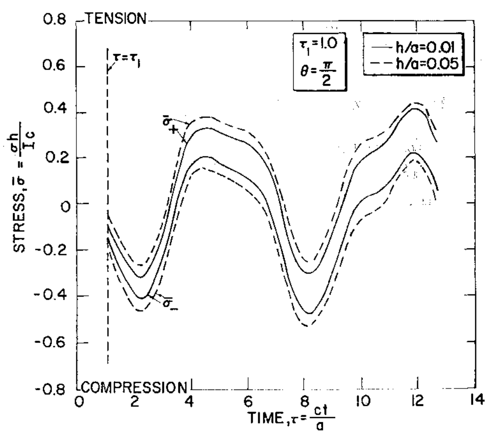

Fig. 7 Computed cylinder response, finite pulse time, ($\theta = \pi/2, 3\pi/2$).

Table 1 Response at small pulse times

θ	τ	Stress	$\tau_1 = 0$	$\tau_1 = 0.0001$	$\tau_1 = 0.001$	$\tau_1 = 0.01$	$\tau_1 = 0.1$
0	$\frac{3\pi}{8}$	$\bar{\sigma}_+$	−0.70089	−0.70090	−0.70097	−0.70146	−0.70513
		$\bar{\sigma}_-$	−0.70698	−0.70699	−0.70701	−0.70742	−0.70980
	$\frac{5\pi}{4}$	$\bar{\sigma}_+$	0.38408	0.38411	0.38432	0.38581	0.40036
		$\bar{\sigma}_-$	0.41969	0.41969	0.41971	0.42053	0.42854
	$\frac{15\pi}{4}$	$\bar{\sigma}_+$	0.28390	...[a]	0.28391	...[a]	...[a]
		$\bar{\sigma}_-$	0.54863	...[a]	0.54843	...[a]	...[a]
π	π	$\bar{\sigma}_+$	−0.42257	−0.42257	−0.42259	−0.42287	−0.41949
		$\bar{\sigma}_-$	−0.37982	−0.37981	−0.37975	−0.37905	−0.37619
	$\frac{13\pi}{8}$	$\bar{\sigma}_+$	−0.61484	0.61483	0.61465	0.61295	0.60130
		$\bar{\sigma}_-$	0.73473	0.73473	0.73470	0.73435	0.72372
	$\frac{5\pi}{2}$	$\bar{\sigma}_+$	−0.54045	...[a]	−0.54049	...[a]	...[a]
		$\bar{\sigma}_-$	−0.59312	...[a]	−0.59317	...[a]	...[a]

[a] Not computed.

Variation of the stress across the thickness due to bending response is evident in Figs. 4–7 and is seen to represent a relatively small effect, superimposed on a fundamentally extensional oscillation of stress. This variation is most pronounced at $\theta = (\pi/2)$ (see Fig. 5 and 7), where there is a discontinuity in the load distribution, and bending can be expected to play a significant role. At $\theta = 0$ or π, even for relatively thick shells, the inside and outside stress curves remain quite close to the pure membrane case.

The present elastic model contains no dissipation, and some question can legitimately be raised whether the maximum stresses in the time are indeed experienced during the first few cycles shown. As a check on this, one case was run for a much later time $20\pi \leqq \tau \leqq 22\pi$, with results indicating that even over a long period of time, the size of the stress peaks remains about the same and the vibrations remain basically extensional.

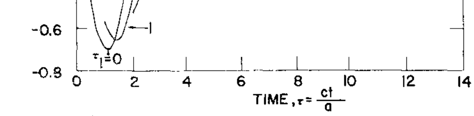

Fig. 8 Comparison of response for different pulse times, ($\theta = 0$).

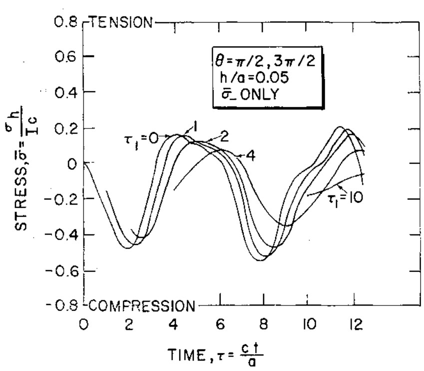

Fig. 9 Comparison of response for different pulse times, ($\theta = \pi/2, 3\pi/2$).

Part of the purpose of this investigation was to study the influence of finite pulse time on linear response compared with impulsive (zero time) loading. For this reason, the form of the solution was set up so that the pulse time could be varied, keeping the total impulse per unit area constant. It was found that the differences in the maximum stress calculations from the case $\tau_1 = 0$ were so small for $\tau_1 = 0.0001$, 0.001, and 0.01 that they could not be seen on an ordinary plot. Even $\tau_1 = 0.1$ is extremely close. Some representative $\bar{\sigma}$ values for these short-time pulses, evaluated at or near the curve peaks, are shown in Table 1. The comparison for longer pulse times is shown in Figs. 8–10, where only the inner surface stress $\bar{\sigma}_-$ for $h/a = 0.05$ is plotted. In general, it is seen that lengthening the pulse lowers and delays the peak stresses, which is to be expected since the applied peak pressure is becoming lower and the energy input is taking place over a longer time. Only the calculation valid for $\tau > \tau_1$ was actually carried out here, so the curve for $\tau_1 = 10$, where difference in response becomes really appreciable, is very curtailed on Figs. 8–10. For long pulses, the alternate calculation for $\tau < \tau_1$ based on Eqs. (28) can be set up.

B. Zero-Impulse Loading

To back up the apparent conclusions from the preceding results for short pulse times, the response to a second type of pulse with equal positive and negative phases (having no net impulse) was considered. The pressure space function is the

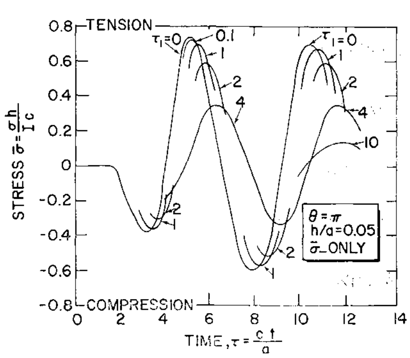

Fig. 10 Comparison of response for different pulse times, ($\theta = \pi$).

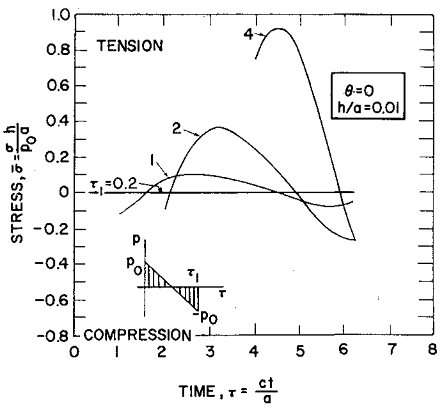

Fig. 11 Comparison of response for different pulse times with zero net impulse.

same as in Fig. 2 and (27), whereas the pressure time function, shown in Fig. 11, is now such that the impulse per unit area (or I) vanishes.

In nondimensional terms, using (6) and (9),

$$P(\tau) = P_0(1 - 2\tau/\tau_1) \qquad 0 \le \tau \le \tau_1$$
$$= 0 \qquad \tau \ge \tau_1 \tag{32}$$

Performing the same operations as in the previous case, but replacing (25) by (32) and using (27) and (32) in (18) and (20), the expressions for $\psi_n(\tau)$, $\zeta_0(\tau)$ and $\zeta_n(\tau)$, are, for $\tau > \tau_1$,

$$\psi_n(\tau) = \frac{na_nP_0}{Q_n}\left[\left(\frac{2 - 2\cos\gamma_n\tau_1}{\gamma_n\tau_1} - \sin\gamma_n\tau_1\right)\frac{\sin\gamma_n\tau}{\gamma_n^2} - \left(1 - \frac{2\sin\gamma_n\tau_1}{\gamma_n\tau_1} + \cos\gamma_n\tau_1\right)\frac{\cos\gamma_n\tau}{\gamma_n^2} - \left(\frac{2 - 2\cos\beta_n\tau_1}{\beta_n\tau_1} - \sin\beta_n\tau_1\right)\frac{\sin\beta_n\tau}{\beta_n^2} + \left(1 - \frac{2\sin\beta_n\tau_1}{\beta_n\tau_1} + \cos\beta_n\tau_1\right)\frac{\cos\beta_n\tau}{\beta_n^2}\right] \tag{33a}$$

$$\zeta_0(\tau) = a_0P_0\left[\left(\frac{2 - 2\cos\tau_1}{\tau_1} - \sin\tau_1\right)\sin\tau - \left(1 - \frac{2\sin\tau_1}{\tau_1} + \cos\tau_1\right)\cos\tau\right] \tag{33b}$$

$$\zeta_n(\tau) = \frac{a_nP_0}{Q_n}\left[\left(\frac{2 - 2\cos\gamma_n\tau_1}{\gamma_n\tau_1} - \sin\gamma_n\tau_1\right)\left(\frac{n^2}{\gamma_n^2} - 1\right) \times \sin\gamma_n\tau - \left(1 - \frac{2\sin\gamma_n\tau}{\gamma_n\tau_1} + \cos\gamma_n\tau_1\right)\left(\frac{n^2}{\gamma_n^2} - 1\right)\cos\gamma_n\tau - \left(\frac{2 - 2\cos\beta_n\tau_1}{\beta_n\tau_1} - \sin\beta_n\tau_1\right)\left(\frac{n^2}{\beta_n^2} - 1\right)\sin\beta_n\tau + \left(1 - \frac{2\sin\beta_n\tau_1}{\beta_n\tau_1} + \cos\beta_n\tau_1\right)\left(\frac{n^2}{\beta_n^2} - 1\right)\cos\beta_n\tau\right] \tag{33c}$$

Substituting these into (23) with (27)

$$\bar{\sigma}_{\pm} \equiv \frac{h}{p_0a}\,\sigma_{\pm h/2} = \frac{1}{\pi}\left(\pm\frac{h}{2a} - 1\right) \times \left[\left(\frac{2 - 2\cos\tau_1}{\tau_1} - \sin\tau_1\right)\sin\tau - \left(1 - \frac{2\sin\tau_1}{\tau_1} + \cos\tau_1\right)\cos\tau\right] - \frac{1}{4}\left[\left(\frac{2 - 2\cos 2^{1/2}\tau_1}{2^{1/2}\tau_1} - \sin 2^{1/2}\tau_1\right)\sin 2^{1/2}\tau - \left(1 - \frac{2\sin 2\tau^{1/2}\tau_1}{2^{1/2}\tau_1} + \cos 2^{1/2}\tau_1\right)\cos 2^{1/2}\tau\right]\cos\theta - \frac{2}{\pi}\sum_{n=2,4,6\ldots}^{\infty}\frac{(-1)^{n/2}}{Q_n(n^2 - 1)}\,[q_{n\pm}(A_{2n}\sin\gamma_n\tau - A_{1n}\cos\gamma_n\tau) - r_{n\pm}(B_{2n}\sin\beta_n\tau - B_{1n}\cos\beta_n\tau)]\cos n\theta \tag{34}$$

where

$$A_{1n} = 1 - \frac{2\sin\gamma_n\tau_1}{\gamma_n\tau_1} + \cos\gamma_n\tau_1$$
$$B_{1n} = 1 - \frac{2\sin\beta_n\tau_1}{\beta_n\tau_1} + \cos\beta_n\tau_1$$
$$A_{2n} = \frac{2 - 2\cos\gamma_n\tau_1}{\gamma_n\tau_1} - \sin\gamma_n\tau_1$$
$$B_{2n} = \frac{2 - 2\cos\beta_n\tau_1}{\beta_n\tau_1} - \sin\beta_n\tau_1$$

and $q_{n\pm}$, $r_{\pm}$, γ_n, β_n, and Q_n are as used in Eqs. (30) and (19).

These surface stresses have been computed to $n = 400$ as before, for thickness ratios $h/a = 0.01, 0.05$, positions $\theta = 0, \pi/2, \pi$, pulse durations $\tau_1 = 0.01, 0.2, 1, 2, 4$, and times $0 \le \tau \le 2\pi$. The results for $\theta = 0, h/a = 0.01$ and several values of pulse duration time are plotted in Fig. 11. There is no significant bending for these values of h/a and θ, and therefore only one curve for each τ_1 is shown ($\bar{\sigma}_+ \doteq \bar{\sigma}_-$). It is seen that there is no significant response for τ_1 less than 0.2 for this zero impulse loading. For greater values of τ_1, the response grows rapidly. It is interesting that the curve for $\tau_1 = 4$ shows a larger response than the corresponding case for the single phase pulse. This can be explained as a type of resonance effect, in which the period and mode of oscillation of the load are close to a period and mode of free vibration of the shell. The cylinder of Fig. 11 behaves virtually as a membrane, and examination of the frequency γ_n for a membrane ($h/a = 0$, $\beta_n = 0$) shows that the first few periods of free vibration are $\tau = 6.28$, 4.45, and 2.71. These values correspond to $n = 0$, 1, and 2, respectively, where n is the number of whole waves around the circumference, and check with those obtained by Love[5] for a ring. The higher mode shapes are very different from the applied pulse and are less likely to be excited. Figure 11 indicates that the case $\tau_1 = 4$ is close enough to the resonance condition to cause the peak stress to be twice that of the free vibration case of Fig. 6 at comparable times.

IV. Conclusions

A general conclusion that can be drawn from these results is that, for pressure pulses of length τ_1 less than 0.1, the response depends only on the total impulse and is essentially independent of the pulse shape. Another conclusion is that, away from load discontinuities, bending effects enter only as a small perturbation of a basically extensional vibration, and only for relatively thick shells. Thus, for h/a less than 0.01, a pure membrane solution gives very close results for early time stresses. The particular type of pressure distribution used here is, of course, a relatively smooth one, without any jumps, and it is quite possible that a more localized type of loading will show more pronounced effects of bending and finite pulse time.

Results are presented here only for stresses, but displacements can be readily found by inserting the appropriate terms in Eqs. (28) or (29) into the series expressions (13). With somewhat greater effort, local strain and curvature change could then be found from basic strain-displacement relations.

V. References

[1] Flugge, W., *Stresses in Shells* (Springer-Verlag, Berlin, 1960), p. 219.

[2] Goodier, J. N. and McIvor, I. K., "The elastic cylindrical shell under nearly uniform radial impulse," J. Appl. Mech. **31**, 259 (1964).

[3] Erdelyi, A. (ed.),, *Tables of Integral Transforms* (McGraw-Hill Book Co., Inc., New York, 1954), Vol. 1, pp. 131, 231.

[4] Payton, R. G., "Dynamic membrane stresses in a circular elastic shell," J. Appl. Mech. **28**, 417 (1961).

[5] Love, A. E. H., *Treatise on the Mathematical Theory of Elasticity* (Dover Publications, New York, 1944), p. 454.